Available online at www.sciencedirect.com
ScienceDirect
Trans. Nonferrous Met. Soc. China 24(2014) 3316−3323
Transactions of Nonferrous Metals Society of China
www.tnmsc.cn

Mechanical properties of anti-seepage grouting materials for heavy metal contaminated soil

Yu-you YANG[1], Jian-qiang WANG[2], Hai-jun DOU[1]

1. School of Engineering and Technology, China University of Geosciences (Beijing), Beijing 100083, China;
2. Yunnan Geological Engineering Investigation Design and Research Institute, Kunming 650041, China

Received 10 July 2013; accepted 20 January 2014

Abstract: Cement-based composite grouting materials were used to construct grouting cutoff wall for heavy metal contaminated soil in non-ferrous metal mining areas. Cement, fly ash, and slag as principal ingredients were mixed with water glass in different ways to produce three composite grouting materials. In order to investigate the effect of water glass mixing ratio, Baume degree, fly ash and slag contents on the mechanical properties of the composite grouting materials, particularly their gel time and compressive strength, the beaker-to-beaker method of gel time test and unconfined compressive strength test were conducted. In addition, the phase composition and microstructure of the composite grouting materials were analyzed by the X-ray diffraction (XRD) and scanning electron microscope (SEM) techniques. The test results show that their gel time increases when water glass mixing ratio and Baume degree increase. The gel time increases dramatically when fly ash is added, but decreases slightly if fly ash is partly replaced by slag. When the mixing ratio of water glass is below 20%, their compressive strength increases with the increases of the ratio; when the ratio is above 20%, it significantly decreases. The compressive strength also tends to increase as Baume degree increases, and improves if fly ash and slag are added.

Key words: heavy metal contaminated soil; composite grouting material; gel time; compressive strength; microstructure

1 Introduction

China is a major producer of non-ferrous metals in the world. Its production of ten types of non-ferrous metals in 2013 alone reached 40 million tons [1]. However, massive metal production brings about amounts of tailings. Statistics shows that there are over 300 government-owned non-ferrous metals mine tailings dams across China, with a whopping 2.2 billion tons of tailings in storage [2]. If left untreated or disposed improperly, the wastes will cause significant damage to the environment and ecosystems. One of the major environmental hazards thereof is heavy metal contamination of groundwater and soil, most noticeably by aluminum, lead, zinc, and copper which are the highest in concentration [3]. Contaminated water and soil can affect plants and impair human health via the food chain [4,5]. Therefore, preventing contamination of heavy metals in non-ferrous metal mine tailings should be a top priority in the management of mining operations.

To date, several approaches have been developed to remove heavy metals from contaminated soils, including isolation, immobilization, toxicity reduction, physical separation and extraction [6]. The widely utilized cement solidification/stabilization method works by restricting the migration of contaminants using binders and then reducing their leachability through chemical reactions [7]. It involves complicated physical and chemical processes. Another two methods are phytoremediation and bioremediation, but they usually take a long time to take effect and besides, related technologies are not so well developed [6]. Electrokinetic soil remediation is effective as well, but its application is time-consuming, highly demanding of soil acidic conditions and likely to cause secondary pollution [8,9].

Grouting cutoff wall is also a preferable pollution

Foundation item: Projects (41472278, 41202220) supported by the National Natural Science Foundation of China; Project (20120022120003) supported by the Research Fund for the Doctoral Program of Higher Education, China; Project (51900265647) supported by the Beijing Higher Education Young Elite Teacher Project, China; Project (2652012065) supported by the Fundamental Research Funds for the Central Universities, China

Corresponding author: Yu-you YANG; Tel: +86-10-82322628; E-mail: yangyuyou@cugb.edu.cn

DOI: 10.1016/S1003-6326(14)63472-5

control method in non-ferrous metal mining [10−12]. When grouts are grouted into the contaminated soil, a physical barrier that can impede further movement of contaminants and prevent pollution is built. This method is efficient and especially important in case of water inrush or flooding during mining [13]. Studies of grouting as a means of pollution control are large in number, but over the years finding innovative and high-performance grouts has aroused increasing interest among engineers [14]. The traditional two-fluid grout is composed of cement grout and water glass (sodium silicate) solutions. Recently, introduction of fly ash into the cement grout has been proposed and its feasibility in grouting by a variety of methods has been confirmed [15]. A blended grout containing steel slag, slag and fly ash was suggested by some researchers [16]. Other alternatives for cement, such as clay, bentonite and other industrial residues, have also been examined [17−19].

In this work, a grout made of cement, fly ash and slag was mixed with water glass solution to form a composite grouting material that is environment friendlier and more cost-effective. Mechanical characteristics of this composite grouting material were investigated, but special attention was paid to factors influencing its gel time controllability and compressive strength.

2 Test materials

The test materials include: 1) 45.2-grade Portland cement, with a specific surface area of 370 m^2/kg, 2) class-II fly ash, with a specific surface area of 516 m^2/kg, 3) slag, with a specific surface area of 448 m^2/kg, and 4) 45 °Be′ water glass with a modulus of 2.6. The grain size distribution and chemical constituents of cement, fly ash, and slag are given in Table 1 and Table 2, respectively. Different mixtures of cement, fly ash and slag were mixed with water to produce grouts No. 1, No. 2, and No. 3, with 3% sodium bentonite as the suspending agent and 1% naphthalene plasticizer as the water reducing agent. Details of the grout ingredients and their mixing ratios are given in Table 3. The composite grouting materials were produced by mixing the three grouts with water glass solution.

3 Gel performance test

The beaker-to-beaker method was adopted to measure the gel time of the composite grouting materials. The detailed test procedures are as follows.

Some of No. 1 grout and some of water glass solution were transferred into two separate beakers. The grout was poured into the water glass beaker, and then the mixture was quickly poured back into the grout beaker. The pouring operation was thus repeated and alternated between the two beakers until the mixed grout stopped flowing when the beaker was inclined at about 45°. The gel time of No. 1 grout is defined as the time period from the moment No. 1 grout and water glass were mixed to the moment the mixed grout stopped flowing. This method was also applied to No. 2 and No. 3 grouts. In this manner, the effects of water glass mixing ratio, Baume degree, fly ash and slag content on gel time were determined.

3.1 Effects of water glass mixing ratio on gel time

Water glass of several mixing ratios was taken to measure the gel time of No. 1, No. 2 and No. 3 grouts. Water glass in this set of tests had a modulus of 2.6 and a density of 35 °Be′. The test results are shown in Fig. 1.

Table 1 Grain size distribution of cement, fly ash and slag

Raw material	Grain size/μm							
	0−2.40	2.40−4.97	4.97−10.28	10.28−21.28	21.28−34.56	34.56−44.04	44.04−56.13	>56.13
Cement	11.51	9.95	17.63	30.85	19.37	5.95	3.19	1.55
Fly ash	21.74	19.09	15.95	17.24	11.68	5.12	4.18	5.00
Slag	15.69	13.89	22.92	33.07	13.08	1.26	0.09	0

Table 2 Chemical constituents of cement, fly ash and slag

Raw material	Mass fraction/%							
	SiO_2	Al_2O_3	Fe_2O_3	CaO	MgO	SO_3	Loss	f-CaO
Cement	22.61	4.35	2.46	62.60	1.91	2.89	1.74	0.71
Fly ash	57.62	28.59	4.21	3.46	0.64	0.40	5.78	0.35
Slag	33.84	11.68	2.2	38.13	10.61	1.98	2.56	0.05

Table 3 Mixing ratios of grouting materials

Sample	Mass fraction of cement/%	Mass fraction of fly ash/%	Mass fraction of slag/%	Water-to-cement ratio	Density/(g·cm^{-3})
No. 1	100	−	−	0.8	1.55
No. 2	40	60	−	0.8	1.48
No. 3	40	45	15	0.8	1.46

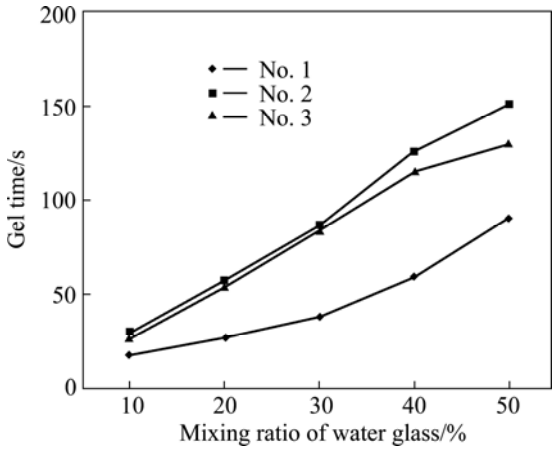

Fig. 1 Effect of water glass mixing ratio on gel time of three grouts

As shown in Fig. 1, the gel time of all the three grouts increases with increasing mixing ratio of water glass. The gel time of No. 1, No. 2, and No. 3 grouts grows by 72, 121 and 103 s, respectively, when the water glass mixing ratio increases from 10% to 50%. Analysis suggests that the rising trend is due to the fact that the density of water glass is lower than that of the three grouts. As the mixing ratio of water glass increases, the three grouts are, in effect, diluted by the water glass solution. This is equivalent to increasing the water-to-cement ratio of the grouts, which enlarges the space between grout particles and increases the time taken to connect the hydration-generated gelatinous substances as a whole. For this reason, the gel time keeps increasing.

3.2 Effects of Baume degree on gel time

Water glass of several Baume degrees was used to measure the gel time of No. 1, No. 2 and No. 3 grouts. Water glass used in the tests had a mixing ratio of 20% and a modulus of 2.6. The test results are shown in Fig. 2.

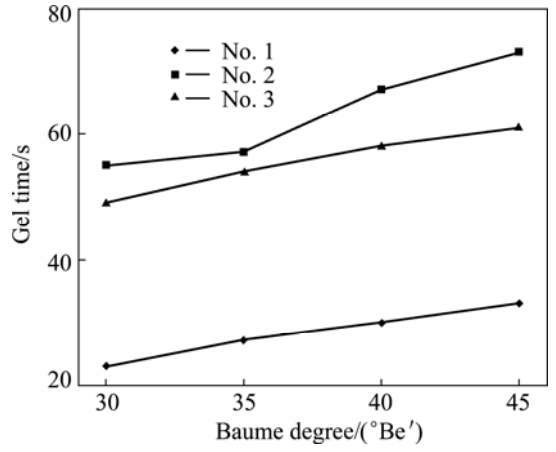

Fig. 2 Effect of Baume degree on gel time of three grouts

Figure 2 suggests that gel time of the three grouts increases as the Baume degree increases, albeit slowly. The gel time of No. 1, No. 2 and No. 3 grouts increases by 43%, 32% and 24%, respectively, as the Baume degree rises from 30 °Be′ to 45 °Be′.

3.3 Effects of powder makeup on gel time

It can be deduced from Fig. 1 and Fig. 2 that the addition of fly ash into the grout markedly increases its gel time. The data of No. 1 and No. 2 grouts show that: as the mixing ratio of water glass increases from 10% to 50%, the gel time of the two grouts increases from 18 s to 90 s and from 30 s to 151 s, respectively; when the Baume degree rises from 30 °Be′ to 45 °Be′, the gel time of the two grouts increases from 23 s to 33 s and from 55 s to 73 s, respectively. When fly ash is partly substituted by slag, gel time of the grout decreases slightly, as indicated by the comparison of No. 2 and No. 3 grouts.

Analysis suggests that in No. 1 grout, calcium ions produced from cement hydration can react immediately with water glass, so that the grout has a relatively short gel time. As fly ash is less active and lower in CaO content than cement, its reaction with water is slower and its hydration products are less. For this reason, if cement is partly substituted by fly ash, as in the case of No. 2 grout, the gel time will be significantly prolonged. Slag is more active and higher in CaO content than fly ash. Although CaO in slag cannot dissolve as quickly as those in cement, the glass particles in it can be gradually broken up by OH^- and meanwhile calcium ions will be gradually released into the solution. Therefore, if fly ash is partly substituted by slag, the calcium ions in the solution will increase accordingly, and their reaction with silicate ions produced in water glass hydration will naturally speed up. With more hydration products, the gel time decreases accordingly.

4 Compressive strength tests of composite grouting materials

Grouts No. 1, No. 2, and No. 3 were separately mixed with water glass, and then the fully mixed grouts were cast into molds of 70.7 mm×70.7 mm×70.7 mm. The cast blocks are hereafter referred to as test blocks a, b and c, respectively. The test blocks were demolded 24 h later and cured under standard conditions for 3 d and 28 d for the unconfined compressive strength test.

4.1 Effects of water glass mixing ratio on compressive strength

The compressive strengths of test blocks b and c, produced by mixing No. 2 and No. 3 grouts with 10%, 20%, 30%, 40% or 50% water glass, were tested at 28 d of curing. Water glass had a modulus of 2.6 and a density of 35 °Be′. The test results are shown in Fig. 3.

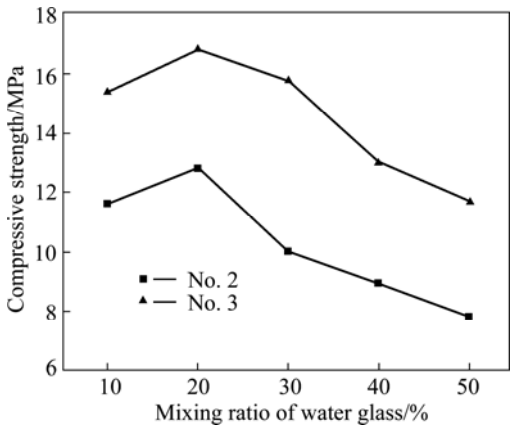

Fig. 3 Effect of water glass mixing ratio on compressive strength of test blocks

The test results shown in Fig. 3 suggest that there is an optimum water glass mixing ratio. When the mixing ratio is low, the compressive strength of test blocks b and c increases with the increase of the ratio. Their compressive strengths hit a peak at the ratio of 20%, but decline immediately and sharply afterwards when the ratio continues to grow. As the mixing ratio increases from 20% to 50%, their compressive strengths decrease by 39.1% and 30.4%, respectively.

Analysis suggests that in the case of low water glass mixing ratios, the hydration products that water glass activates fly ash and slag to produce are insufficient, resulting in a low compressive strength of the test blocks. In the case of high water glass mixing ratios, excessive water glass produces silicic acid gels of low strength. Moreover, water in water glass solution can dilute the whole system, which, in effect, is not different from raising the water-to-cement ratio of the grout. This invariably affects the overall compressive strengths of the test blocks. On the other hand, the hydration of water glass produces large quantities of $[H_nSiO_4]^{x-}$, which reacts with Ca^{2+} in the solution and produces not only calcium silicates hydrates (C-S-H) but also silica sols. Silica sols, however, have low strength, thus triggering a decrease in the overall strength of the test blocks. Consequently, only a proper water glass mixing ratio can ensure sufficient production of C-S-H and zeolite-like materials with low CaO/SiO_2 ratio, which can give the test blocks a high compressive strength. Given the test results presented above, 20% is proposed as the optimum mixing ratio of water glass.

4.2 Effects of Baume degree on compressive strength

The compressive strengths of test blocks b and c, produced by mixing No. 2 and No. 3 grouts with water glass of 30 °Be′, 35 °Be′, 40 °Be′, and 45 °Be′, were tested at 28 d curing. Water glass had a mixing ratio of 20% and a modulus of 2.6. The test results are shown in Fig. 4.

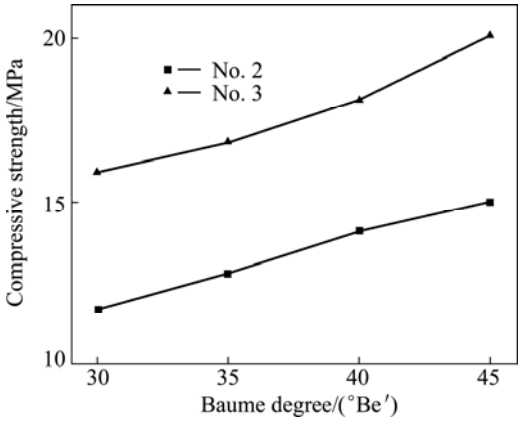

Fig. 4 Effect of Baume degree on compressive strength of test blocks

It can be readily seen from Fig. 4 that the compressive strengths of the two test blocks tend to increase with increasing Baume degree. As the Baume degree increases from 30 °Be′ to 45 °Be′, the compressive strengths of test blocks b and c increase by 28% and 27%, respectively. Analysis suggests that at a fixed water glass mixing ratio, the production of $[SiO_3]^{2-}$ in water glass hydration increases with the increase in Baume degree. These ions react with Ca^{2+}, producing more C-S-H and thus enhancing the compressive strength of the test blocks.

4.3 Effects of fly ash and slag on compressive strength

Grouts No. 1, No. 2 and No. 3 were mixed with water glass and cured under standard conditions, producing test blocks a, b and c. The unconfined compressive strengths of the test blocks were tested at 3 d and 28 d curing. Water glass used in this set of tests had a mixing ratio of 20%, a density of 35 °Be′ and a modulus of 2.6. The test results are shown in Fig. 5.

It can be deduced from the comparison of test blocks a and b that if cement in grout is partly replaced

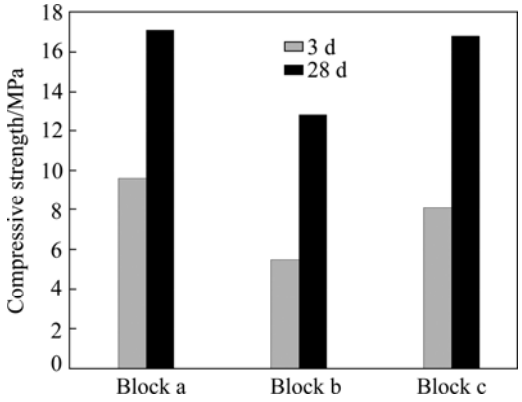

Fig. 5 Effect of powder makeup on compressive strength of test blocks

by fly ash, the compressive strengths of the test block at 3 d and 28 d will both experience a marked decrease. Nonetheless, test block c made of cement-fly ash-slag mixed grout has a considerably enhanced compressive strength. At 28 d, it is almost equal to that of test block a, and at 3 d, it is still larger than that of test block b. Due to its relatively weak activity, most fly ash hardly engages in the early phase of hydration, which results in reduced production of C-S-H within the system and a low compressive strength of the test block. For this reason, cement-fly ash mixed grout cannot achieve the most desirable grouting effect. By contrast, the mixed grout made of cement, fly ash, and slag can do so. For one thing, slag can readily engage in the early phase of hydration due to its better activity than fly ash, generating large quantities of C-S-H, so that the compressive strength is enhanced. For another, mixing powders of different fineness can improve the gradation of the particle system, so that the spaces between particles are better filled and particles get more closely packed. Compactness of the whole system is enhanced, and so its compressive strength is improved.

5 X-ray diffraction analysis

Grouts No. 1, No. 2, No. 3 and 20% water glass were mixed to prepare test blocks a, b, and c. The test blocks were analyzed using the XRD technique. The XRD patterns of cement, fly ash and slag are shown in Fig. 6 and those of the test blocks at 3 d and 28 d curing are shown in Figs. 7 and 8, respectively.

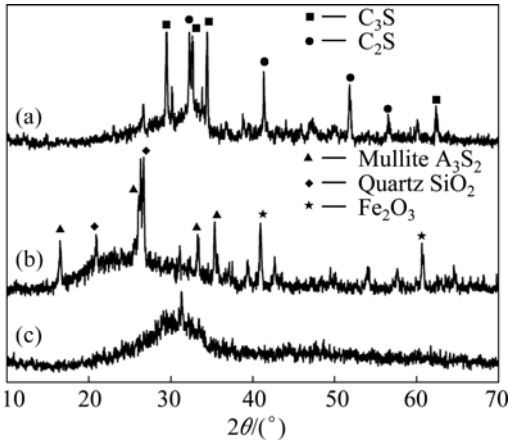

Fig. 6 XRD patterns of cement (a), fly ash (b), and slag (c)

It can be seen from Figs. 7 and 8 that the XRD patterns of the three test blocks all show an obvious $CaCO_3$ diffraction peak. Carbonate calcium comes from $Ca(OH)_2$ carbonization. The XRD pattern of test block a shows an obvious $Ca(OH)_2$ diffraction peak at 3 d and 28 d curing, while the $Ca(OH)_2$ diffraction peaks for test blocks b and c are indistinct. This difference is due to the

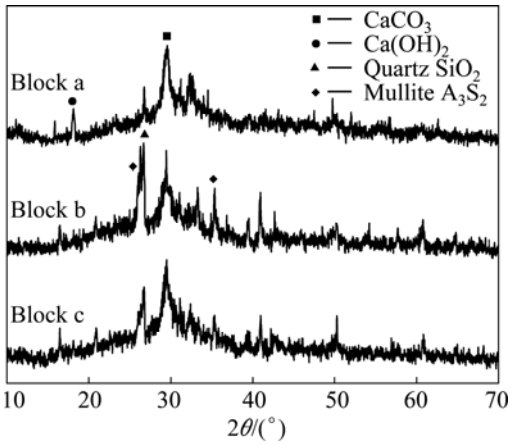

Fig. 7 XRD patterns of composite grouting materials (3 d curing)

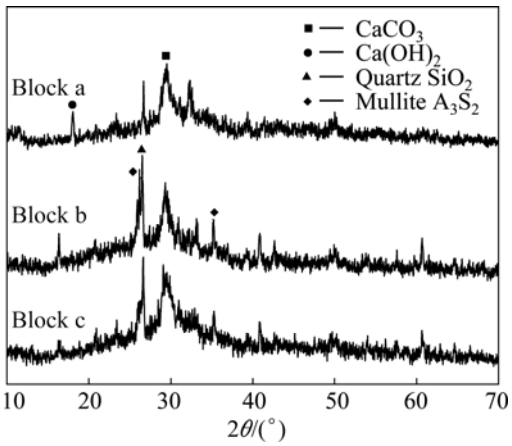

Fig. 8 XRD patterns of composite grouting materials (28 d curing)

changes induced by replacing part of cement by fly ash and slag. On the one hand, the production of $Ca(OH)_2$ decreases as the cement content decreases. On the other hand, part of the $Ca(OH)_2$ generated is consumed to activate fly ash and slag. The XRD pattern of test block b shows distinct diffraction peaks of mullite A_3S_2 and quartz SiO_2 introduced by fly ash. As the curing age grows, however, their diffraction peaks remain almost unchanged. This suggests that inert mullite and quartz crystals in fly ash basically do not engage in the reactions at 28 d. The XRD pattern of test block c between 20° and 40° shows that the bun-shaped diffuse peak at 28 d is evidently much higher than that at 3 d. This suggests that more amorphous gels are generated as the curing age grows. If the XRD patterns of test blocks a and c at 28 d are compared, it can be found that the breadth of the bun-shaped diffuse peak for test block c is clearly larger than that for test block a. This suggests that under alkaline condition, the composite grouting materials produce not only C-S-H gels but also other new amorphous gels.

6 Scanning electron microscope analysis

The SEM images of the test blocks at curing ages of 3 d and 28 d are shown in Fig. 9.

It can be learned from Fig. 9 that at 3 d curing, large quantities of hydration products can be found in test block a, mostly $Ca(OH)_2$ crystals of hexagonal-platelet morphology and reticular type-II C-S-H. Calcium hydroxide has good crystal shape, but $Ca(OH)_2$ and C-S-H overlap each other, making the microstructure loose. In test block b made of cement-fly ash grout, there are substantially less hydration products than in test block a as a result of reduction in total cement use. The smooth-surface spherical fly ash particles suggest that fly ash does not engage in the reactions and merely fills the pores. Fly ash and the hydration products are of loose formation, revealing that their reaction in test block b is less complete than that in test block a. In test block c cast by cement-fly ash-slag mixed grout, massive slag hydration has initiated, but its microstructure remains loose.

At 28 d curing, all the test blocks have a more compact microstructure relative to that at 3 d curing. It can be observed in the SEM image of test block a that $Ca(OH)_2$ crystals and C-S-H gels grow fully and closer together. The C-S-H gels are generated in so large a quantity that no distinct pores can be identified in the microstructure. There are evidently more hydration products in test blocks b and c at 28 d than at 3 d. Pores are better filled by hydration products, so their microstructures get more compact. The spherical fly ash particles are covered by a small amount of hydration products. Fly ash in glass phase begins to hydrate when

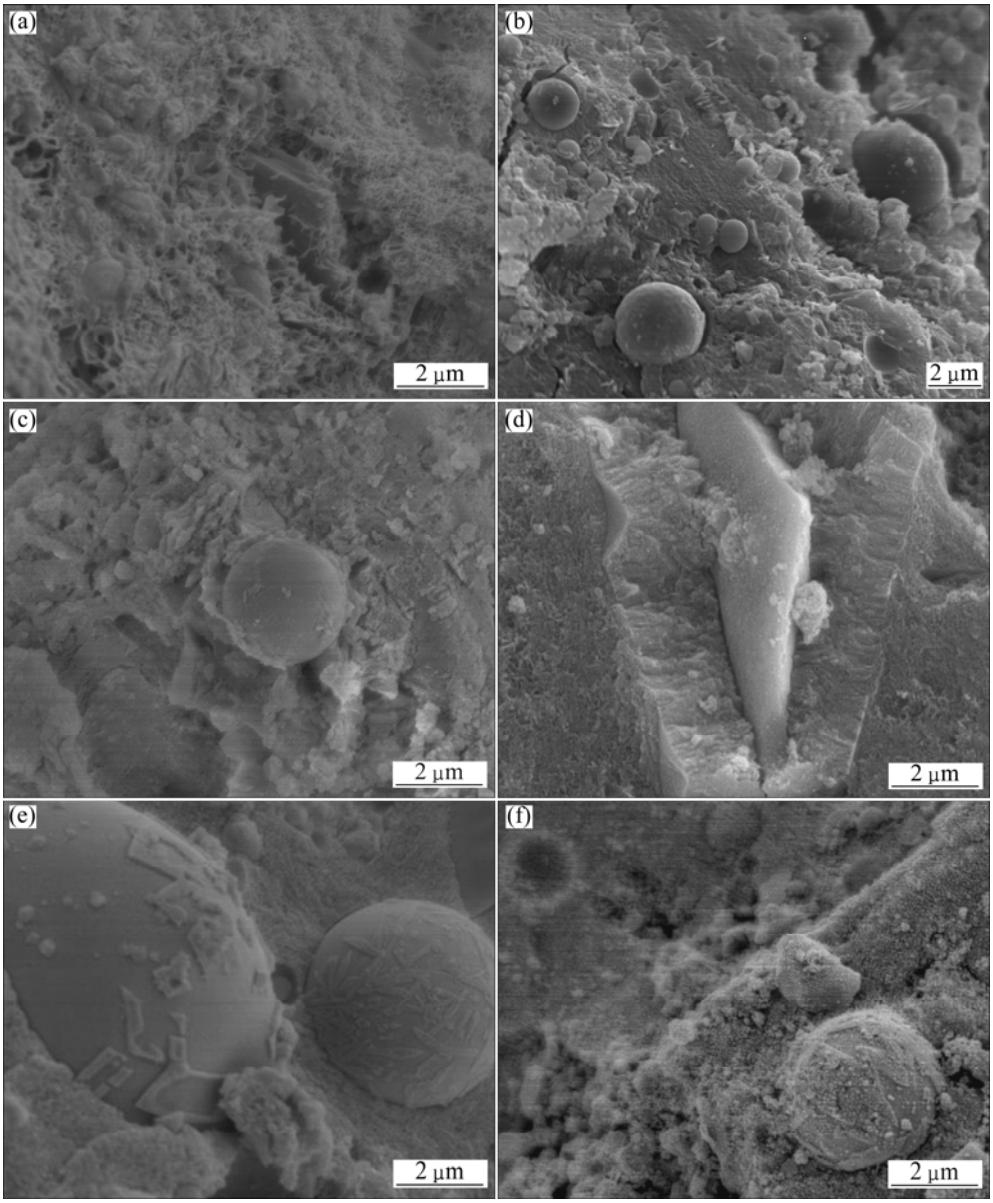

Fig. 9 SEM images of composite grouting materials: (a) Test block a, 3 d; (b) Test block b, 3 d; (c) Test block c, 3 d; (d) Test block a, 28 d; (e) Test block b, 28 d; (f) Test block c, 28 d

activated by alkaline, but its extent of reaction is low on a whole. Larger fly ash particles still have a smooth surface and show no sign of hydration. As slag has better activity than fly ash, no distinct slag particles can be observed in test block c at 28 d.

7 Conclusions

1) Water glass mixing ratio, Baume degree, fly ash and slag contents all have an impact on the gel time of the composite grouting materials. The gel time of No. 1, No. 2 and No. 3 grouts increases with increasing water glass mixing ratio; as the Baume degree increases, their gel time likewise tends to increase, albeit slowly; the gel time increases if cement in grouts is partly substituted by fly ash, and remains so if the content of fly ash increases; with a fixed cement content, a grout will have a slightly reduced gel time if fly ash in it is partly substituted by slag.

2) Water glass mixing ratio, Baume degree, fly ash and slag content all make a strong impact on the compressive strength of the grouting materials. If water glass mixing ratio is less than 20%, their compressive strength increases as the mixing ratio increases; if the mixing ratio is more than 20%, their compressive strength radically decreases; if it is around 20%, they will get their maximum strength; their compressive strength increases gradually with the increase in Baume degree; the test results of test block b show that the introduction of fly ash into the grouting materials can reduce their compressive strengths; addition of slag can substantially improve the strength of test block c.

3) The XRD patterns and SEM images show that in test block a, large quantities of hydration products are generated in the early phase of hydration, when $Ca(OH)_2$ and C-S-H crystals overlap each other but the overall microstructure remains loose. In the later stage, $Ca(OH)_2$ and C-S-H crystals get closer, resulting in a more compact microstructure. By contrast, test blocks b and c produce only a small amount of hydration products in the early stage, when fly ash remains inactive and slag just begins to hydrate. In the final stage, large quantities of hydration products are found in areas around fly ash, indicating that fly ash has been activated by alkaline and begins to hydrate.

References

[1] DUAN S P, GUO M. The situation of non-ferrous metals mining in China in 2013 [J]. China Mining Magazine, 2014, 23: 5−7. (in Chinese)

[2] SUN Y, LIU H F, LIU J M, MENG F W, ZHANG W Q. Current problems in the disposal of non-ferrous metallic tailings [J]. Metal Mine, 2009, 5: 6−10, 15. (in Chinese)

[3] LIU J X, WANG Q, SUN P, GU X W, LI G J. Ecological footprint of China's non-ferrous metal industries [J]. Resources Science, 2007, 29: 155−159. (in Chinese)

[4] SIDENKO N V, KHOZHINA E I, SHERRIFF B L. The cycling of Ni, Zn, Cu in the system "mine tailings–ground water–plants": A case study [J]. Applied Geochemistry, 2007, 22: 30−52.

[5] CHENG S P. Heavy metal pollution in China: Origin, pattern and control [J]. Environmental Science and Pollution Research, 2003, 10: 192−198.

[6] MULLIGAN C N, YONG R N, GIBBS B F. Remediation technologies for metal-contaminated soils and groundwater: An evaluation [J]. Engineering Geology, 2001, 60: 193−207.

[7] BARNETT F, LYNN S, REISMAN D. Technology performance review: Selecting and using solidification/stabilization treatment for site remediation [R]. Cincinnati: U.S. Environmental Protection Agency, 2009.

[8] VIRKUTYTE J, SILLANPÄÄ M, LATOSTENMAA P. Electrokinetic soil remediation–critical overview [J]. Science of the Total Environment, 2002, 289: 97−121.

[9] PAGE M M. Electroremediation of contaminated soils [J]. Journal of Environmental Engineering, 2002, 128: 208−219.

[10] LIU J, YU B, JI Z N, CHEN H. Application of grout curtain and penetration resistance technology in in-situ leaching [J]. Nonferrous Metals, 2003, 55: 112−123, 129. (in Chinese)

[11] XUE Q, LI J S, LIU L. Experimental study on anti-seepage grout made of leachate contaminated clay in landfill [J]. Applied Clay Science, 2013, 80−81: 438−442.

[12] CHEN Y G, ZOU Y S, ZHANG K N, DENG F Y. Heavy metals transport process through clay-solidified grouting curtain in waste landfills [J]. Rock and Soil Mechanics, 2007, 28: 2583−2588. (in Chinese)

[13] BANKS D, YOUNGER P L, ARNESEN R F, IVERSEN E R, BANKS S B. Mine-water chemistry: The good, the bad and the ugly [J]. Environmental Geology, 1997, 32: 157−174.

[14] SHI C J, JIMÉNEZ A F, PALOMO A. New cements for the 21st century: The pursuit of an alternative to Portland cement [J]. Cement and Concrete Research, 2011, 41: 750−763.

[15] CHEN L Y, WANG S. Research and application of fly ash grouting material [J]. Journal of Chengdu University of Technology: Science & Technology Edition, 2007, 34: 206−209. (in Chinese)

[16] ZHANG G Z, DING Q J. Research and application of a two-component grouting material with sodium silicate and industrial residue [J]. Modern Tunnelling Technology, 2007, 44: 79−84. (in Chinese)

[17] AKBULUT S, SAGLAMER A. Evaluation of fly ash and clay in soil grouting [C]//Proceedings of the Third International Conference on Grouting and Ground Treatment. New Orleans: ASCE, 2003: 1192−1199.

[18] ZHANG K N, CHEN Y G, DENG F Y, TIAN Q Y. Retention of clay-solidified grouting curtain to Cd^{2+}, Pb^{2+} and Hg^{2+} in landfill of municipal solid waste [J]. Journal of Central South University of Technology, 2004, 11(4): 419−422.

[19] KACI A, CHAOUCHE M, ANDRÉANI P A. Influence of bentonite clay on the rheological behaviour of fresh mortars [J]. Cement and Concrete Research, 2011, 41(4): 373−379.

重金属污染土防渗注浆材料的力学性能

杨宇友[1]，王建强[2]，豆海军[1]

1. 中国地质大学(北京) 工程技术学院，北京 100083；
2. 云南地质工程勘察设计研究院，昆明 650041

摘　要：采用水泥基复合注浆材料对有色金属矿区重金属污染土进行防渗隔离处理。水泥、粉煤灰和矿渣等主要材料分别以不同组分与水玻璃混合形成 3 种复合注浆材料。采用倒杯法试验、无侧限抗压强度试验等方法研究不同水玻璃掺量、波美度以及粉煤灰和矿渣掺量对复合注浆材料凝胶时间和抗压强度等力学性能的影响规律。此外，采用 XRD 和 SEM 等测试方法，从材料的物相组成及微观结构方面进一步分析了复合注浆材料的力学特性。研究结果表明：凝胶时间随着水玻璃掺量和波美度的增大而延长；粉煤灰可以显著延长凝胶时间，但使用矿渣代替部分粉煤灰会使凝胶时间略有减少。当水玻璃掺量在 20%以下时，复合注浆材料抗压强度随着水玻璃掺量的增加而增加，当水玻璃掺量超过 20%，抗压强度显著降低；抗压强度随波美度的增加而增大；粉煤灰和矿渣可提高复合注浆材料的抗压强度。

关键词：重金属污染土；复合注浆材料；凝胶时间；抗压强度；微观结构

(Edited by Yun-bin HE)